

Transcriptional profiles of rock bream iridovirus (RBIV) using microarray approaches

Myung-Hwa Jung^{*}, Jun-Young Song^{**} and Sung-Ju Jung^{***†}

^{*}Department of Marine Bio and Medical Sciences, Hanseo University, Seosan, Republic of Korea

^{**}Pathology Division, National Institute of Fisheries Science, Busan, Republic of Korea

^{***}Department of Aquaculture Medicine, Chonnam National University, Yeosu, Republic of Korea

Rock bream iridovirus (RBIV) causes high mortality and economic losses in the rock bream (*Oplegnathus fasciatus*) aquaculture industry in Korea. Viral open reading frames (ORFs) expression profiling at different RBIV infection stages was investigated using microarray approaches. Rock bream were exposed to the virus and held for 7 days at 23 °C before the water temperature was reduced to 17 °C. Herein, 28% mortality was observed from 24 to 35 days post infection (dpi), after which no mortality was observed until 70 dpi (end of the experiment). A total of 27 ORFs were significantly up- or down-regulated after RBIV infection. In RBIV-infected rock bream, four viral genes were expressed after 2 dpi. Most RBIV ORFs (26 genes, 96.2%) were significantly elevated between 7 and 20 dpi. Among them, 12 ORF (44.4%) transcripts reached their peak expression intensity at 15 dpi, and 14 ORFs (51.8%) were at peak expression intensity at 20 dpi. Expression levels began to decrease after 25 dpi, and 92.6% of ORFs (25 genes) were expressed below 1-fold at 70 dpi. From the microarray data, in addition to the viral infection, viral gene expression profiles were categorized into three infection stages, namely, early (2 dpi), middle (7 to 20 dpi), and recovery (25 and 70 dpi). RBIV ORFs 009R, 023R, 032L, 049L, and 056L were remarkably expressed during RBIV infection. Furthermore, six ORFs (001L, 013R, 052L, 053L, 058L, and 061L) were significantly expressed only at 20 dpi. To verify the cDNA microarray data, we performed quantitative real-time PCR, and the results were similar to that of the microarray. Our results provide novel observations on broader RBIV gene expression at different stages of infection and the development of control strategies against RBIV infection.

Key words: rock bream, rock bream iridovirus, microarray, viral gene expression, virus replication

Introduction

Iridoviridae is a family of large double-stranded DNA viruses (120~300 nm) with an icosahedral morphology (Williams *et al.*, 1996). The family includes five genera, namely *Iridovirus*, *Chloriridovirus*, *Ranavirus*, *Lymphocystivirus*, and *Megalocytivirus*. Rock

bream iridovirus (RBIV) infection is a major viral disease resulting from a virus of the genus *Megalocytivirus* (Kurita and Nakajima, 2012), which causes high mortality in rock bream (*Oplegnathus fasciatus*) (Jung and Oh, 2000). RBIV is known for its high pathogenicity against rock bream (Jung *et al.*, 2015; Jung *et al.*, 2016; Jung *et al.*, 2017a; Jung and Jung, 2017a; Jung *et al.*, 2017b; Jung *et al.*, 2019; Jung and Jung, 2019; Jung and Jung, 2021). Once activated, RBIV is not easily inactivated in the rock bream body (Jung

†Corresponding author: Sung-Ju Jung
Tel: +82-61-659-7175; Fax: +82-61-659-7179
E-mail: sungju@chonnam.ac.kr

et al., 2017b). Moreover, to date, the response of the immune defense system of rock bream under RBIV infection remains unclear, and hence, it remains an important health risk. A considerable number of studies have been conducted to reveal the immune responses of rock bream at both physiological and molecular levels using proteomic and microarray analyses (Kwon *et al.*, 2013; Jung *et al.*, 2018; Kim *et al.*, 2020). Recently, several studies have focused on the transcriptional immune responses of rock bream against RBIV (Jung *et al.*, 2014; Nikapititya *et al.*, 2014; Jung and Jung, 2017b; Jung and Jung, 2017c; Jung and Jung, 2017d). However, most studies have focused on the major organ-mediated immune responses to determine the pathway responsible for fish mortality or survival.

The genome of RBIV (NCBI accession number AY532606) is 112,080-bp-long and contains at least 118 putative open reading frames (ORFs) (Do *et al.*, 2004). Viral envelope membrane protein ORF007L (major capsid protein, MCP) related studies are well known. The MCP gene has been used to detect and assess RBIV infection (Jung *et al.*, 2015; Jung *et al.*, 2016), and it is the main immunogenic protein of *Megalocytivirus* (Caipang *et al.*, 2006; Fu *et al.*, 2014). Although we found that rock bream administered with viral envelope membrane protein ORF008L (myristoylated membrane protein, MMP) and ORF094R (ANK-containing protein, ANK)-based DNA vaccine and exposed to RBIV showed the highest protective effect (Jung *et al.*, 2018; Jung *et al.*, 2022), the role of most RBIV ORFs was unclear. This indicates that a lack of viral genomic-related experiments is severely hampering further advancement in revealing specific information to elucidate the pathogenic mechanisms underlying RBIV infection. Therefore, evaluation of the viral gene transcriptional profile over the time-course of RBIV infection will be useful to understand the host-RBIV interactions.

DNA microarray technology has been used to explore viral gene expression patterns of mammalian

and piscine viruses under different conditions in animal models. This approach provides valuable information for understanding and discovering gene functions and gene expression profiles and detecting specific genes that respond to pathogens in fish (Thanasaksiri *et al.*, 2015; Cho *et al.*, 2016; Romero *et al.*, 2015). To date, microarrays have been used to study the viral DNA expression in fish infected with *Megalocytivirus* (red seabream iridovirus; RSIV) (Lua *et al.*, 2005; Lua *et al.*, 2007) and *Ranavirus* (singapore grouper iridovirus; SGIV) (Teng *et al.*, 2008). Lua *et al.* (Lua *et al.*, 2005; Lua *et al.*, 2007) developed a DNA microarray containing 92 putative ORFs of RSIV, and the viral gene transcription programs of RSIV were examined in HINAE cells (olive flounder natural embryo) *in vitro* and in infected red seabream (*Pagrus major*) *in vivo*. A DNA microarray was developed containing 127 predicted ORFs of SGIV to investigate the SGIV ORF expression profiles in grouper embryo cells (Teng *et al.*, 2008). However, viral gene expression changes in rock bream after RBIV infection have not been comprehensively analyzed using microarray approaches.

In the present study, our goal was to investigate the viral gene expression profiles over time against RBIV infection to better understand the pathogenic mechanisms of RBIV infection at the transcriptional level. We constructed a DNA microarray containing probes for 27 putative RBIV ORFs and examined RBIV genome transcription profiles over the time-course of the disease in a rock bream model *in vivo*. Moreover, the microarray results were further validated using qRT-PCR.

Materials and methods

RBIV infection and sample preparation

RBIV was isolated from the spleen and kidney of RBIV-infected rock bream in 2010 (Jung *et al.*, 2014). The spleen and kidney were homogenized with nine volumes of DMEM (Dulbecco's Minimum Essential

Medium) (Gibco, USA) and centrifuged at 737 g for 20 min at 4 °C. The supernatants were subdivided and used for the challenge study. RBIV-free rock bream were obtained from a local farm. The major capsid protein (MCP) gene copies of the original RBIV in the supernatant preparations, quantified by using quantitative real time polymerase chain reaction PCR (qRT-PCR) as $7.5 \times 10^7/100 \mu\text{L}$. It was suspended in PBS to 1.1×10^7 , 1.2×10^6 , and $6.7 \times 10^5/100 \mu\text{L}$, as previously described (Jung et al., 2014). All rock bream experiments were conducted in strict accordance with the recommendations of the Institutional Animal Care and Use Committee of Chonnam National University (permit number: CNU IACUC-YS-2016-3).

The artificial experimental method was explained previously (Jung and Jung, 2017b). A total of 60 fishes ($34.1 \pm 2.1 \text{ g}/11.7 \pm 1.7 \text{ cm}$) was intraperitoneally (i.p.) injected with 100 μl of RBIV at a concentration of 1.1×10^7 MCP gene copies per fish. Control fish were injected with the same volume of phosphate-buffered saline (PBS). Experimental fish were maintained in tanks supplied with 250 L of UV-treated seawater at 23 °C for 7 days, and the water temperature was shifted to 17 °C (by 2 °C/d). Because rock bream injected with RBIV and held at 23 °C rapidly exhibited 100% mortality and no mortality was observed at 17°C in an earlier study (Jung and Jung, 2017b), the water temperature for the experimentally infected rock bream was shifted from 23 °C to 17°C (during the very early stages of infection) to reduce mortality. Therefore, in the present study, we investigated the viral gene expression patterns in the different stages of infection (early, middle, and recovery), which might be necessary to identify important responses for viral inhibition/replication.

Five fish were randomly chosen from each group at 2, 7, 10, 15, 20, 25, and 70 days post infection (dpi). The head kidney and spleen were collected and stored at -80 °C. One fish sample from each sampling point was used for microarray experiments. Five fish

samples from each group and time point were used for qRT-PCR evaluation.

Microarray analysis

The cDNA microarray used in this study contained more than 22,940 unique probes. Microarray interrogations were performed using a custom-designed, Agilent-based microarray platform with $8 \times 60 \text{ K}$ probes per slide. The microarray used in this study was designed using 60-mer probes for 22,866 probes using eArray software, and the microarrays were manufactured using Agilent Technologies (USA). For control and test RNAs, the synthesis of target cRNA probes and hybridization were performed using the Low RNA Input Linear Amplification kit (Agilent Technology) according to the manufacturer's instructions. Total RNA was prepared from each sample, and a sample of 0.2 μg of qualified RNA was labeled with Cy5 (virus-infected sample) and Cy3 (PBS-injected control sample). cDNA was hybridized onto the microarray chips for 17 h at 65 °C using an Agilent Hybridization oven (Agilent Technology). The hybridization images were obtained using an Agilent DNA Microarray Scanner G2505C (Agilent Technology), and the data quantification was analyzed using Agilent Feature Extraction Software 9.3.2.1 (Agilent Technology). All data normalization and selection of fold-changed genes were performed using GeneSpring Software GX 7.3.1 (Agilent Technology). Logged gene expression ratios were normalized using the locally weighted regression scatterplot smoothing (LOWESS) method. The averages of normalized ratios were calculated by dividing the average normalized signal channel intensity by the average of normalized control channel intensity. ORFs with >2-fold changes were selected and considered significant ORFs.

Validation of the microarray results using qRT-PCR

To validate the microarray results, real-time PCR

Table 1. The list of primers used in this study

Name	Sequence (Forward)	Sequence (Reverse)	Accession number
ORF004	GTGATGGCACGTATCGTTGC	ACACCAGGCACACTGTACAC	AAT71819
ORF007	TGCACAATCTAGTTGAGGAGGTG	AGGCGTTCCAAAAGTCAAGG	AY849394
ORF023	GTGCTGTCCAGTTGGCTACT	CCGGTGGACAGCTTGTACAT	AAT71838
ORF032	TAAAACGGTGCCTCAGGTCC	ACTCGACAGGCAAATGCTGA	AAT71847
ORF048	ATTGGAGTACAGCGACACCC	AACGCCGTGCACTTCATTTTC	AAT71863
ORF094	CCCAGCTCTACCACAAGCAA	GTCATGCACAAAGCTGGCAA	AAT71909
ORF099	GCATTTCCAACCTGCCATGCA	GGTGAAGACGAGCAAGGTGA	AAT71914

was performed using an AccuPre®2x Greenstar qPCR Master Mix (Bioneer, Korea) in an Exicycler 96 Real-Time Quantitative Thermal Block (Bioneer). Briefly, real-time PCR was conducted with specific RBIV ORFs primers (Table 1). Total RNA was extracted from the head kidney using the RNAiso Plus reagent (TaKaRa, Japan), following the standard protocol recommended by the manufacturer. Any remaining genomic DNA was digested using DNase I (TaKaRa) according to the manufacturer's protocol. Synthesis of cDNA was performed using a Rever Tra Ace qPCR RT Kit (Toyobo, Japan). Each assay was performed in duplicate using β -actin RNA as control. The relative expression of each gene was determined using the $2^{-\Delta\Delta Ct}$ method (Livak and Schmittgen, 2001). Statistical analyses of the expression levels of immune genes were performed using unpaired t-tests with the GraphPad Prism software version 5.0 for Windows (GraphPad Software, USA). A value of $p < 0.05$ and $p < 0.01$ indicated statistical significance.

Quantification of RBIV using qRT-PCR

The spleen is one of the organs where RBIV replication occurs. Hence, the RBIV MCP gene is easily detected in the spleen after RBIV infection (Jung and Oh, 2000; Jung *et al.*, 2015; Jung and Jung, 2017a). To measure the absolute RBIV copy number, genomic DNA was extracted from whole spleen (20~150 mg) samples using an AccuPrep® Genomic DNA extraction kit (Bioneer) according to the manufacturer's protocol. The method for developing a standard curve followed that described previously

(Jung *et al.*, 2014). The results are presented as the total number of virus copies per 1 μ l of genomic DNA taken from 100 μ l of total genomic DNA. Statistical analyses were performed using GraphPad Prism software version 5.0. A one-way analysis of variance (ANOVA) was performed between conditions with Tukey's multiple comparison test. A value of $p < 0.05$ was considered statistically significant.

Results and Discussion

RBIV disease progression in rock bream

Rock bream were experimentally infected via i.p. injection with RBIV. Specifically, mortality was observed after 24, 25, 26, 27, and 35 dpi (one fish per day) with an estimated cumulative mortality of 4, 8, 13, 18, and 28%, respectively. Then, no mortality was observed until 70 dpi (end of the experiment) (Fig. 1A).

RBIV MCP copies were detected using spleen samples and qRT-PCR at all sampling points (2, 7, 10, 15, 20, 25, and 70 dpi) in rock bream (Fig. 1B). The early phase of infection was at 2 dpi, and viral transcription was $2.20 \times 10^0/\mu$ l. The acute stage of RBIV infection occurred from 7 to 20 dpi, at 7, 10, 15, and 20 dpi, the virus copy numbers increased and were 6.86×10^5 , 2.21×10^6 , 1.19×10^5 , and $1.37 \times 10^7/\mu$ l, respectively. The virus copy numbers then decreased after 25 dpi ($5.98 \times 10^3/\mu$ l). These time points (after 25 dpi) were regarded as the sub-acute stage of RBIV infection. After 70 dpi, the recovery stage of infection, the virus was reduced to under the negative de-

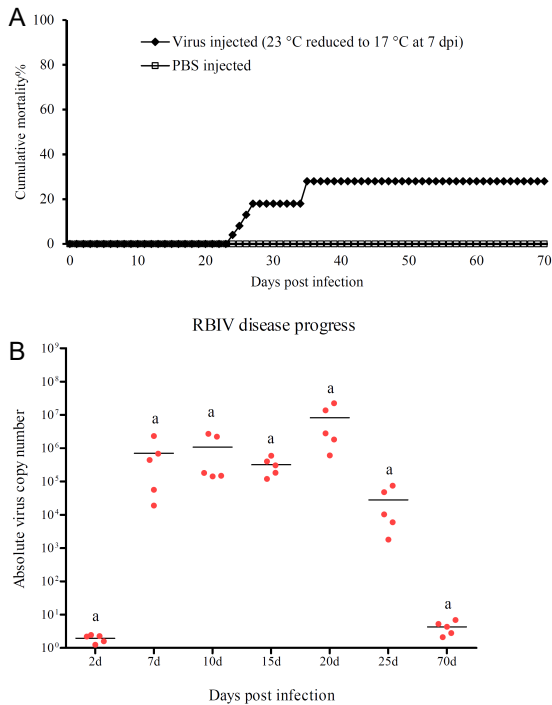


Fig. 1. Rock bream were intraperitoneally (i.p.) injected with RBIV (1.1×10^7 MCP gene copies/100 μ l/fish): virus infection at 23 °C reduced to 17 °C at 7 dpi. (A) Mortality was calculated using the formula: $[(\text{number of dead fish}/\text{fish population parameter}) \times 100]$. (B) Changes of absolute virus copy numbers in rock bream. One-way analysis of variance (ANOVA) was performed between conditions with Tukey's multiple comparison test. Different superscript letters denote significant differences ($P < 0.05$). Data are represented as individual values. The line represents the mean value. The experimental groups, published previously [15, 17], are shown for reference.

tection level of $2.20 \times 10^0/\mu$ l.

RBIV transcription in virus-infected rock bream head kidneys using microarray approaches

1) Three infection stages of RBIV transcripts

The RBIV transcription profiles were constructed and are presented in Table 2. They totaled 27 viral genes that were up- or down-regulated after RBIV infection (Figs. 2 and 3). At 2, 7, 10, 15, 20, 25, and 70 dpi, up-regulated (over 2-fold) gene numbers were

4 (14.8%), 5 (18.5%), 13 (48.1%), 18 (66.6%), 24 (88.8%), 1 (3.7%), and 1 (3.7%), respectively (Table 2 and Fig. 3). As shown in Table 2, 44.4% (12 genes) of transcripts reached their peak expression intensity at 15 dpi, whereas 51.8% (14 genes) reached peak expression intensity at 20 dpi. Only 3.7% (1 gene) transcripts reached their maximum expression at 70 dpi. From the microarray data, the viral gene expression profiles were categorized into three infection stages, namely, early (2 dpi), middle (7 to 20 dpi), and recovery (25 and 70 dpi) (Fig. 3).

(1) Early stage of infection

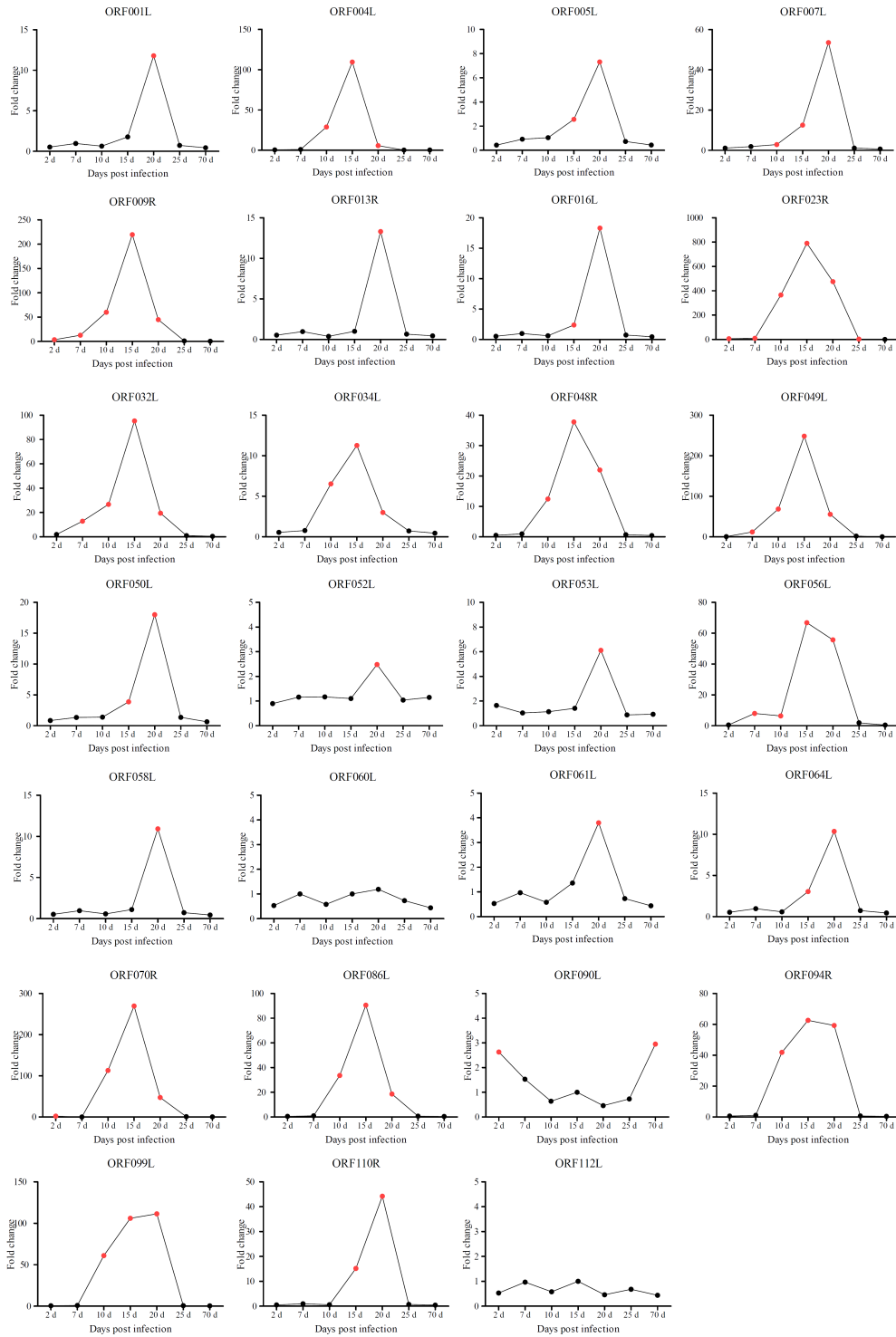
At the early stage of infection at 2 dpi, the infected fish appeared grossly healthy, and the number of infectious agents began to increase. Four viral genes were up-regulated, namely, ORF009R hypothetical protein, ORF023R laminin-type epidermal growth factor-like domain, ORF070R hypothetical protein, and ORF090L hypothetical protein (Table 2, Fig. 4, and Supplementary Fig. 1)

(2) Middle stage of infection

The middle stage of the disease was from 7 to 20 dpi. Thereafter, active replication of the virus and its numbers peaked exponentially, and the fish showed some clinical symptoms.

At 7 dpi, expressed signals of five ORFs were elevated, namely, ORF009R hypothetical protein, ORF023R laminin-type epidermal growth factor-like domain, ORF032L hypothetical protein, ORF049L hypothetical protein, and ORF056L hypothetical protein (Table 2, Fig. 4, and Supplementary Fig. 1).

Along with the virus infection, the number of expressed RBIV ORFs rapidly increased from 10 dpi. At 10 dpi, expressed signals of 13 ORFs were elevated, including ORF004L hypothetical protein, ORF007L MCP, ORF032L hypothetical protein, ORF034L hypothetical protein, ORF070R, ORF094R ankyrin repeat-containing protein, and ORF099L hypothetical protein (Table 2, Fig. 4, and Supplementary Fig. 1).



Supplementary Fig. 1. The RBIV ORF expression levels at 2, 7, 10, 15, 20, 25, and 70 days post RBIV infection. Red circles indicate expression ratios greater than the mean (2-fold up-regulated).

Table 2. Microarray analysis of RBIV transcripts profiles

No.	ORF	Putative function	Accession No.	Time points						
				2 dpi	7 dpi	10 dpi	15 dpi	20 dpi	25 dpi	70 dpi
1	ORF001L	Transmembrane amino acid transporter protein	AAT71816.1	0.53	0.97	0.64	1.78	11.79	0.73	0.44
2	ORF004L	Hypothetical protein	AAT71819.1	0.53	1.02	28.92	109.58	5.85	0.32	0.44
3	ORF005L	Hypothetical protein	AAT71820.1	0.43	0.92	1.05	2.56	7.31	0.73	0.44
4	ORF007L	Major capsid protein	AAT71822.1	1.11	1.86	2.87	12.51	53.53	1.10	0.68
5	ORF009R	Hypothetical protein	AAT71824.1	3.55	12.83	60.15	219.73	44.90	1.05	0.44
6	ORF013R	Serine/threonine protein kinase catalytic domain	AAT71828.1	0.53	0.97	0.38	1.00	13.30	0.66	0.45
7	ORF016L	Hypothetical protein	AAT71831.1	0.53	0.97	0.60	2.37	18.31	0.73	0.44
8	ORF023R	Laminin-type epidermal growth factor-like domain	AAT71838.1	5.96	9.86	365.41	790.03	475.64	2.71	0.55
9	ORF032L	Hypothetical protein	AAT71847.1	1.96	12.84	26.71	95.28	19.47	1.06	0.44
10	ORF034L	Hypothetical protein	AAT71849.1	0.56	0.78	6.53	11.27	3.00	0.73	0.46
11	ORF048R	Vascular endothelial growth factor-like protein	AAT71863.1	0.53	0.97	12.44	37.79	21.98	0.73	0.44
12	ORF049L	Hypothetical protein	AAT71864.1	0.53	12.05	68.65	248.34	55.59	1.84	0.44
13	ORF050L	Hypothetical protein	AAT71865.1	0.84	1.34	1.40	3.88	18.00	1.36	0.64
14	ORF052L	Hypothetical protein	AAT71867.1	0.90	1.16	1.17	1.10	2.48	1.04	1.15
15	ORF053L	Hypothetical protein	AAT71868.1	1.65	1.04	1.14	1.41	6.11	0.88	0.93
16	ORF056L	Hypothetical protein	AAT71871.1	0.53	7.96	6.36	66.82	55.71	1.93	0.44
17	ORF058L	Putative DNA-binding protein	AAT71873.1	0.53	0.97	0.58	1.11	10.92	0.73	0.44
18	ORF060L	mRNA capping enzyme	AAT71875.1	0.53	1.00	0.58	1.00	1.19	0.73	0.44
19	ORF061L	RING-finger-containing E3 ubiquitin ligase	AAT71876.1	0.53	0.97	0.58	1.36	3.80	0.73	0.44
20	ORF064L	Hypothetical protein	AAT71879.1	0.53	0.97	0.58	3.05	10.36	0.73	0.44
21	ORF070R	Hypothetical protein	AAT71885.1	2.05	0.23	113.00	269.68	47.40	0.77	0.44
22	ORF086L	Hypothetical protein	AAT71901.1	0.53	0.97	33.63	90.56	18.60	0.73	0.44
23	ORF090L	Hypothetical protein	AAT71905.1	2.63	1.53	0.64	1.00	0.46	0.73	2.95
24	ORF094R	Ankyrin repeat-containing protein	AAT71909.1	0.66	1.12	41.93	62.66	59.33	0.73	0.44
25	ORF099L	Hypothetical protein	AAT71914.1	0.53	0.97	61.11	106.02	111.39	0.73	0.44
26	ORF110R	Immediate early protein ICP-46	AGG37989.1	0.53	0.97	0.60	15.17	44.21	0.73	0.44
27	ORF112L	Early 31-kDa protein	AGG37991.1	0.53	0.97	0.58	1.00	0.46	0.68	0.44

Many RBIV ORFs began to elevate at 10 dpi, indicating that intensive replication, transcription, and translation were taking place to assemble and form viral progeny inside infected host cells.

At 15 dpi, 18 ORFs were significantly elevated. Among them, the expression of 12 viral genes reached their peak at 15 dpi and then began to decrease at

20 dpi (Table 2). Furthermore, the up-regulation of approximately 50% (ORFs 004L, 009L, 023R, 049L hypothetical protein, 070R, and 099L) and 33.3% (ORFs 032L, 056L, 086L hypothetical protein, and 094R ankyrin repeat-containing protein) of expressed ORFs were over 100- and 50-fold, respectively, at 15 dpi (Table 2, Fig. 4, and Supplementary Fig. 1).

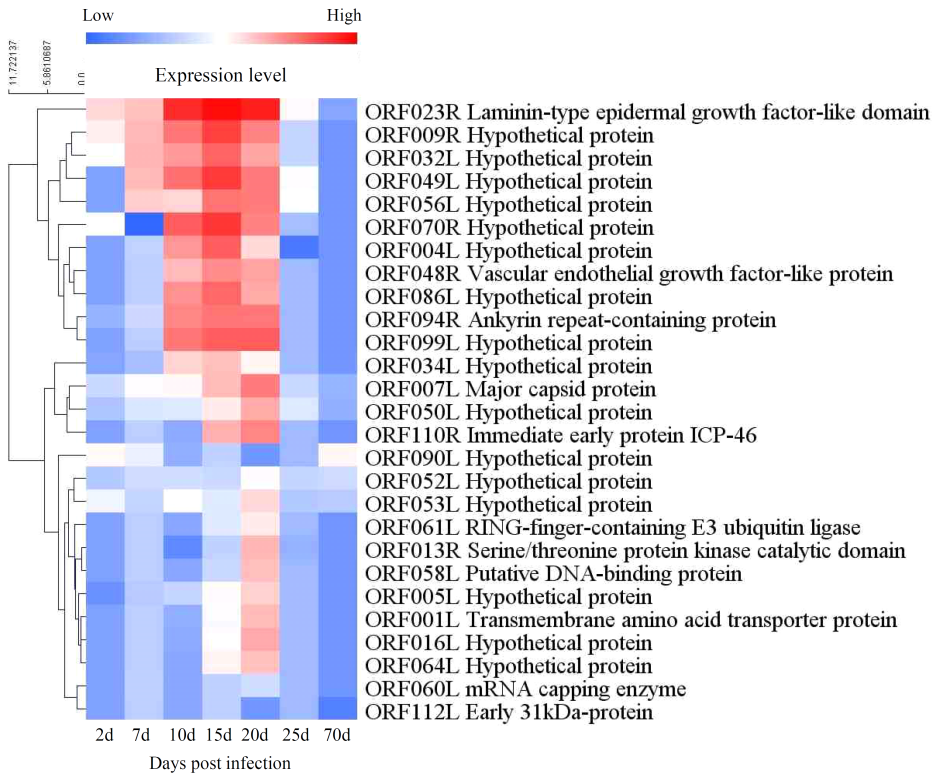


Fig. 2. RBIV ORF cluster analysis of microarray results (2-fold up- or down-regulated) and ORFs expression profiles at 2, 7, 10, 15, 20, 25, and 70 days post RBIV infection. Red boxes indicate expression ratios greater than the mean. White boxes indicate an intermediate level of expression. Blue boxes indicate expression ratios lower than the mean.

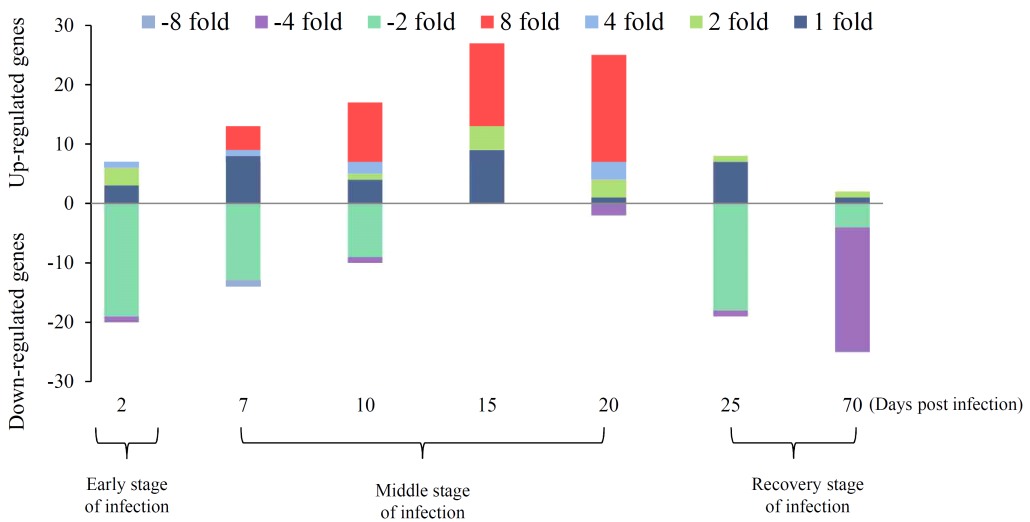


Fig. 3. Distribution of regulated RBIV ORF numbers throughout RBIV infection. Significantly modulated genes are subdivided according to the fold change or regulation level (up or down).

Among the expressed ORFs, ORF094 ankyrin repeat-containing protein, ankyrin repeats, and ankyrin-like repeats were found in various proteins; they are involved in cell cycle, tissue differentiation, gene transcription, and mediating protein–protein interactions (Bennett, 1992). Several viruses, including *Poxviridae*, *Polydnaviridae*, *Phycodnaviridae*, *Mimiviridae*, and *Iridoviridae* families, were found to encode via ankyrin repeat-containing proteins (He *et al.*, 2001; Herbert *et al.*, 2015; Lu *et al.*, 1995; Raoult *et al.*, 2004; Bitra *et al.*, 2012). Moreover, the ankyrin repeat genes are known to play a role against viral infection: i) in the herpes simplex virus-1 (HSV-1) and respiratory syncytial virus (RSV), the ankyrin repeat domain significantly induced interferon-related responses, and overexpression of the ankyrin repeat domain conferred protection in cell lines (Bin *et al.*, 2016); ii) CHOhr contains an ankyrin repeat gene and is involved in the inhibition of virus-induced apoptosis against cowpox virus (Ink *et al.*, 1995); and iii) the 28.2-kD IκB protein homolog contains an ankyrin repeat similar to IκB, which interfered with nuclear factor (NF)-κB activation, demonstrating a mechanism to invade immune responses against African swine fever virus infection (Revilla *et al.*, 1998). Do *et al.* (2004) proposed that in RBIV the ankyrin repeat genes might also play a similar role in mediating viral and host cellular proteins (Do *et al.*, 2004).

At 20 dpi, 24 RBIV ORFs were elevated, including the ORFs for the MCP, and ORF023R, and ORF099L were strongly expressed. This finding indicated that most RBIV virions were completely assembly by 20 dpi (Table 2). Furthermore, the up-regulation of approximately 8.3% (ORFs 023R and 099L) and 16.6% (ORFs 007L, 049L, 056L, and 094R) of expressed ORFs were over 100- and 50-fold, respectively, at 20 dpi. Interestingly, six ORFs (001L transmembrane amino acid transporter protein, 013R serine/threonine-protein kinase catalytic domain, 052L hypothetical protein, 053L hypothetical protein, 058L putative DNA-binding protein, and 061L RING-finger-con-

taining E3 ubiquitin ligase) out of these 24 ORFs were significantly expressed only at 20 dpi (Table 2, Fig. 4, and Supplementary Fig. 1). ORF013R encoded a protein that contained serine/threonine-protein kinase. HSV-1 encodes a serine/threonine kinase (UL13) that is packaged into the virion, and UL13 is essential for its functions in viral penetration of cells and onset of viral protein synthesis by phosphorylating viral proteins (Cunningham *et al.*, 1992; Overton *et al.*, 1992). Moreover, the ORF 061L encoded a protein that contained the RING-finger-containing ubiquitin ligase domain. A viral protein of HSV-1 contains the RING-finger-containing ubiquitin ligase domain, and this region is essential for its function in regulating gene expression, stimulating lytic infection, inducing proteasome-dependent degradation of cellular proteins, and conjugating ubiquitin (Paterson and Everett, 1988). From these findings, it could be suggested that the six ORFs induced resulted in very specific responses when virus replication reached its peak at 20 dpi. Therefore, these RBIV ORFs may have some essential functions in viral gene expression and viral replication.

In the present study, the RBIV MCP gene reached its peak expression at approximately 20 dpi. Similarly, it has been reported that RSIV and SGIV MCP expression were highly elevated at the later stage of infection using microarray approaches (Lua *et al.*, 2007; Teng *et al.*, 2008). Interestingly, we found that the five most highly expressed RBIV ORFs in rock bream occurred in the early and later stage of infection and were more efficiently induced than MCP during RBIV infection. Table 2 presents the up-regulated viral genes, including ORF009R, ORF023R, ORF032L, ORF049L, and ORF056L, which were highly expressed in the middle stage of infection from 7 to 20 dpi, indicating that these viral genes played important roles in viral DNA replication in rock bream. However, some differences between RBIV and RSIV were observed in the ORF expression patterns. In the RSIV microarray analysis results, i) ORF291L and

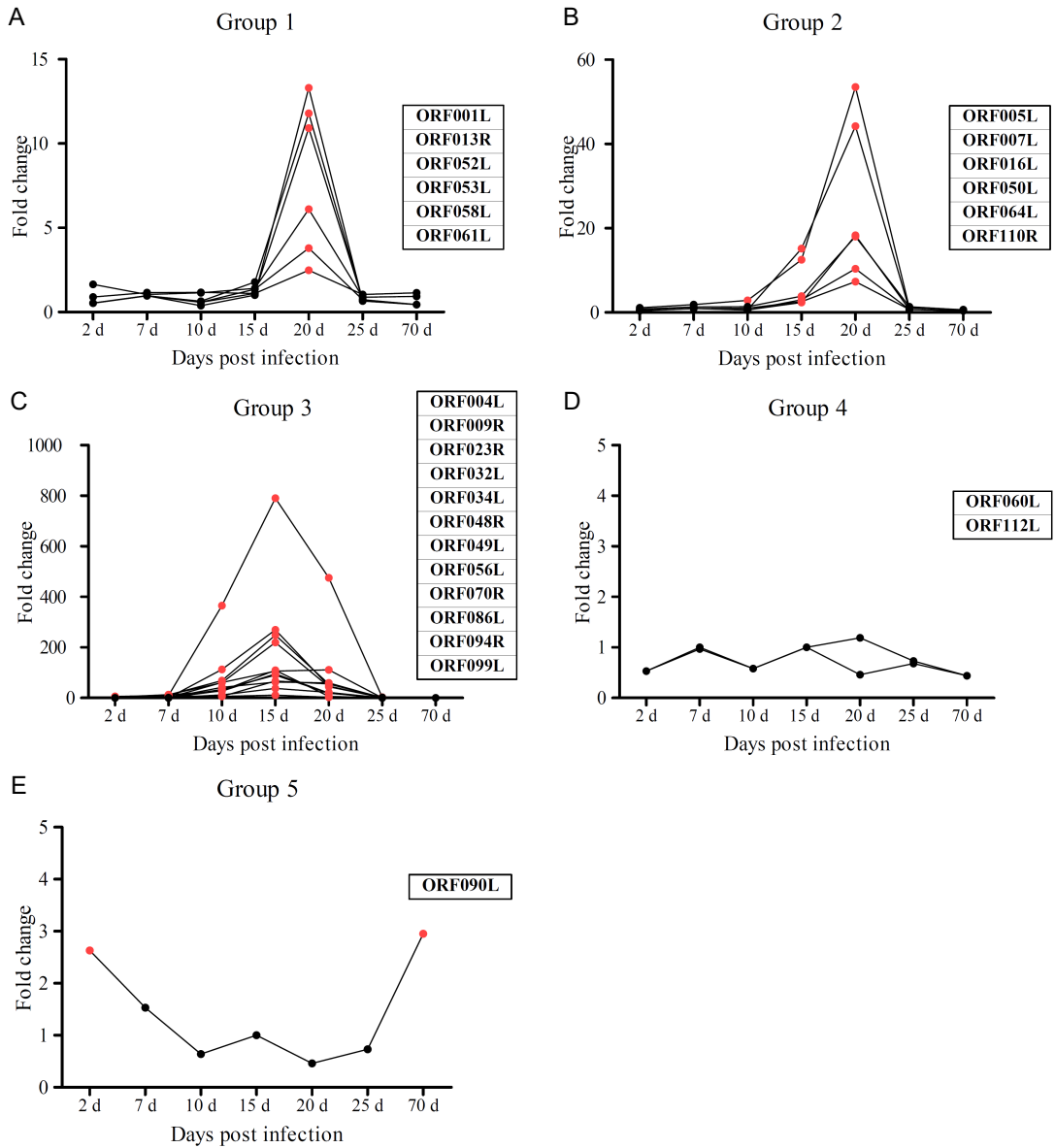


Fig. 4. Time-course expression analysis of five RBIV transcripts classes. Differential RBIV gene expression profiles at 2, 7, 10, 15, 20, 25, and 70 days post RBIV infection. Red circles indicate expression ratios greater than the mean (2-fold up-regulated).

ORF097R, which were expressed more than MCP, with homolog genes being RBIV ORFs 023R and 056L; and ii) ORF226R and ORF128R, which were expressed less than MCP, with homolog genes being RBIV ORFs 032L and 049L (Lua *et al.*, 2007). Hence, the presence of modulated RBIV ORFs in RBIV-in-

ected rock bream is an informative result of this microarray experiment, which yielded a valuable tool for the study of RBIV transcripts. Furthermore, the expression level of these ORFs in the major organs of rock bream may be important in the evaluation of the molecular markers for the relative severity of

RBIV diseases. Interestingly, only ORF023R expression was elevated over 300-fold in RBIV-infected rock bream at 10, 15, and 20 dpi (365.4-, 790-, and 475-fold, respectively). ORF023R contains the laminin-type epidermal growth factor-like domain, and it has been reported that the nidogen-binding site of laminin plays a role in cell-to-cell adhesion (Mayer *et al.*, 1993). A unique function of the laminin-type epidermal growth factor-like domain gene of *Megalocytiviruses*, including RSIV and infectious spleen and kidney necrosis virus (ISKNV), has been reported: i) The specific monoclonal antibody M10 (mAb M10) has been developed as an accurate diagnostic tool to identify RSIV; mAb M10 epitope was found in the laminin-type epidermal growth factor-like domain protein (LEGFD of RSIV) but not in other proteins of RSIV (other 107 ORFs), thereby indicating that LEGFD is the sole target of mAb M10 among RSIV proteins (Takano *et al.*, 2020); and ii) VP23R protein (LEGFD protein of ISKNV) of ISKNV interacts with nidogen-1 to play a pivotal role in the attachment of infected cells to lymphatic endothelial cells, suggesting an immune evasion strategy adopted by *Megalocytiviruses* to effectively shield virus-infected cells from host immune attack before virus virion maturation (Xu *et al.*, 2010; Xu *et al.*, 2014). However, other strongly expressed ORFs (009R, 032L, 049L, and 056L) are of unknown function. Therefore, the details of the ORFs function need to be elucidated in the future and will be interesting subjects of further studies, such as viral gene-based monoclonal antibodies, vaccine development, and diagnosis of RBIV disease.

(3) Recovery stage of infection

The numbers of expressed ORFs began to decrease at 25 dpi (only one gene was highly expressed; ORF023R), and most of the viral genes (92.6%, 25 genes) gradually decreased to below 1-fold by 70 dpi (Table 2 and Figs. 2 and 3), indicating that the viral load started to decline because of the host antiviral immune defense. Hence, this period was regarded as

the recovery stage of infection.

Furthermore, ORF090L showed expression levels dependent on the virus replication pattern. The highest ORF090L expression was observed in the early stage of infection (at 2 dpi, 2.63-fold) that gradually decreased to the basal level by 20 dpi (from approximately 0.46 to 1.53-fold) when most of the viral genes were highly expressed (Table 2 and Fig. 4). Surprisingly, ORF090L expression rebounded at the end of the experiment (at 70 dpi) when most of the viral ORFs (96.2%, 26 genes) were reduced to the minimum (below 1-fold), suggesting that ORF090L expression levels were highly dependent on the virus replication patterns in the microarray data.

Differential RBIV gene expression profiles

All viral transcripts in the kidney of rock bream were clustered into five groups with the similarity of expression patterns as follows: group 1, six ORFs (001L, 013R, 052L, 053L, 058L, and 061L) were significantly expressed only at 20 dpi (Fig. 4A); group 2, six ORFs (005L, 007L, 016L, 050L, 064L, and 110R) were gradually expressed from 15 dpi and reached peak expression at 20 dpi (Fig. 4B); group 3, 12 ORFs (004L, 009R, 023R, 032L, 034L, 048R, 049L, 056L, 070R, 086L, 094R, and 099L) were highly expressed at 10, 15, and 20 dpi (Fig. 4C); group 4, ORFs 060L and 112L were not highly expressed during the infection period (Fig. 4D); group 5, ORF 090L was expressed as early as 2 dpi and then gradually decreased from 7 to 25 dpi and rebounded at 70 dpi (Fig. 4E). These findings could impart an in-depth understanding of the replication mechanism, gene regulation strategies, and pathogenesis of RBIV.

Transcriptional responses using qRT-PCR

We selected seven RBIV ORFs that may play main roles in the viral replication. These ORFs consisted of 004L (hypothetical protein), 007L (MCP), 023R (LEGFD), 032L (hypothetical protein), 048R (vascular endothelial growth factor-like protein), 094R

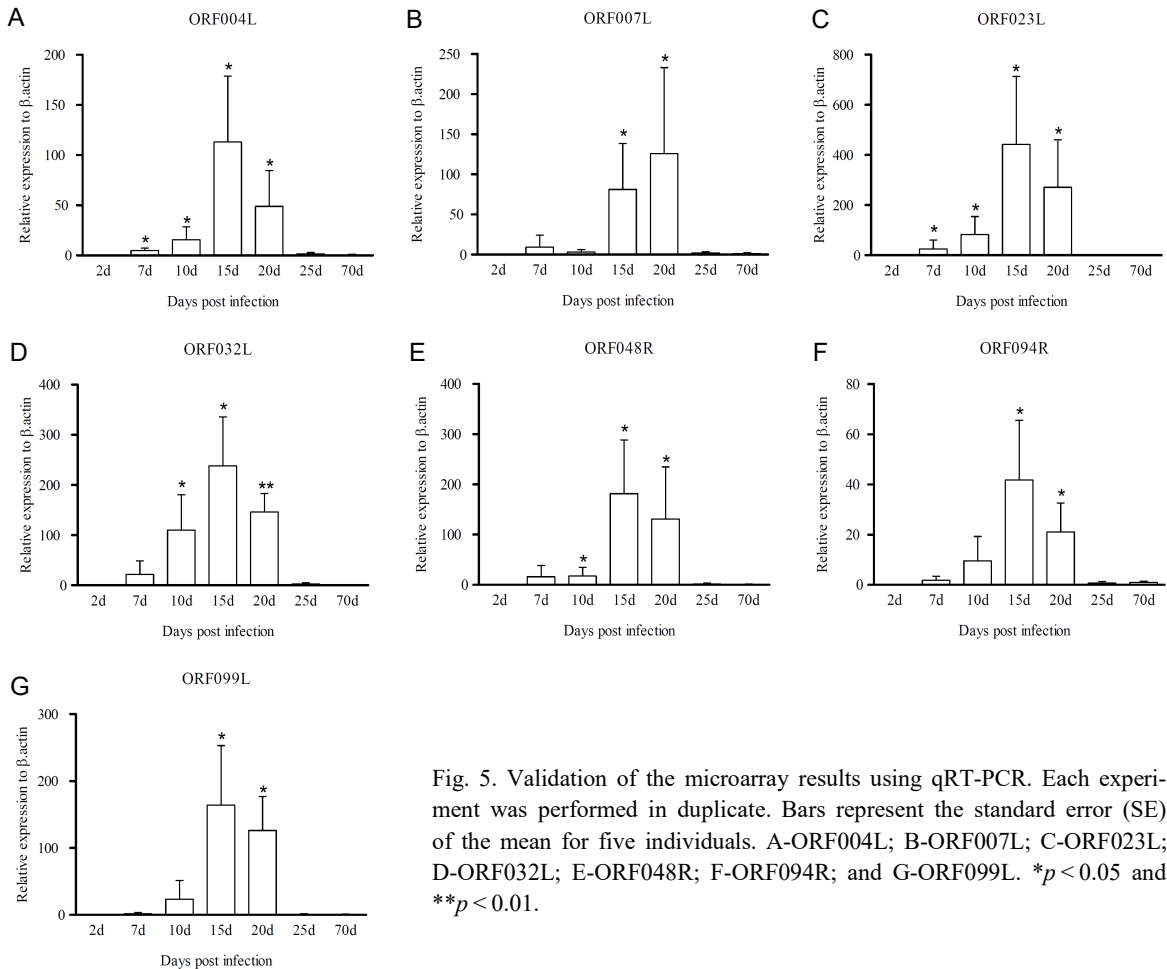


Fig. 5. Validation of the microarray results using qRT-PCR. Each experiment was performed in duplicate. Bars represent the standard error (SE) of the mean for five individuals. A-ORF004L; B-ORF007L; C-ORF023L; D-ORF032L; E-ORF048R; F-ORF094R; and G-ORF099L. * $p < 0.05$ and ** $p < 0.01$.

(ankyrin repeat-containing protein), and 099L (hypothetical protein). Among these, ORF023L and ORF032L were the highest expressed at approximately 400- and 220-fold (at 15 dpi), respectively. As shown Fig. 5, most gene expression profiles were similar to that of the heat map in the overall microarray results (Fig. 2).

Conclusions

To better understand the molecular mechanisms of RBIV pathogenesis, the global expression profiles of RBIV were investigated using a time-course experiment with RBIV-infected rock bream. In conclusion,

the results documented the transcriptional profiles of RBIV-infected rock bream kidneys using microarray approaches. RBIV transcription started as early as 2 dpi, replication began at approximately 7 to 10 dpi, and the virion assembly was processed from approximately 20 dpi in rock bream kidneys. Most of the RBIV ORFs were elevated and reached their peak expression levels at 15 and 20 dpi. Then, the number and expression levels began to decrease after 25 dpi. Our study provides the experimental foundation for further investigation of RBIV infection and pathogenesis mechanisms and will facilitate the development of antibodies, specific diagnostics, and effective virus gene-based vaccines.

Acknowledgments

This research was supported by the National Institute of Fisheries Science, Ministry of Oceans and Fisheries, Republic of Korea (R2022070).

References

- Williams, T.: The Iridoviruses. *Adv Virus Res*, 46: 345-412, 1996.
- Kurita, J. and Nakajima, K.: Megalocytiviruses. *Viruses*, 4: 521-538, 2012.
- Jung, S.J. and Oh, M.J.: Iridovirus-like infection associated with high mortalities of striped beak perch, *Oplegnathus fasciatus* (Temminck et Schlegel), in southern coastal areas of the Korea peninsula. *J Fish Dis*, 23: 223-236, 2000.
- Jung, M.H., Jung, S.J., Vinay, T.N., Nikapitiya, C., Kim, J.O., Lee, J.H., Lee, J. and Oh, M.J.: Effects of water temperature on mortality in *Megalocytivirus*-infected rock bream *Oplegnathus fasciatus* (Temminck et Schlegel) and development of protective immunity. *J Fish Dis*, 38: 729-737, 2015.
- Jung, M.H., Lee, J. and Jung, S.J.: Low pathogenicity of FLIV (flounder iridovirus) and the absence of cross-protection between FLIV and RBIV (rock bream iridovirus). *J Fish Dis*, 39:1325-1333, 2016.
- Jung, M.H., Lee, J., Ortega-Villaizan, M., Perez, L. and Jung, S.J.: Protective immunity against *Megalocytivirus* infection in rock bream (*Oplegnathus fasciatus*) following CpG ODN administration. *Vaccine*, 35: 3691-3699, 2017a.
- Jung, M.H. and Jung, S.J.: Protective immunity against rock bream iridovirus (RBIV) infection and TLR3-mediated type I interferon signaling pathway in rock bream (*Oplegnathus fasciatus*) following poly (I:C) administration. *Fish. Shellfish Immunol*, 67: 293-301, 2017a.
- Jung, M.H., Nikapitiya, C., Vinay, T.N., Lee, J. and Jung, S.J.: Rock bream iridovirus (RBIV) replication in rock bream (*Oplegnathus fasciatus*) exposed for different time periods to susceptible water temperatures. *Fish. Shellfish Immunol*, 70: 731-735, 2017b.
- Jung, M.H. and Jung, S.J.: Correlation of virus replication and spleen index in rock bream iridovirus infected rock bream *Oplegnathus fasciatus*. *J. Fish. Pathol*, 32:1-8, 2019.
- Jung, M.H. and Jung, S.J.: Microsatellite marker distribution pattern in rock bream iridovirus (RBIV) infected rock bream, *Oplegnathus fasciatus*. *J. Fish. Pathol*, 34: 9-15, 2021.
- Jung, M.H., Nikapitiya, C. and Jung, S.J.: DNA vaccine encoding myristoylated membrane protein (MMP) of rock bream iridovirus (RBIV) induces protective immunity in rock bream (*Oplegnathus fasciatus*). *Vaccine*, 36: 802-810, 2018.
- Jung, M.H., Nikapitiya, C., Kim, S.J., Han, H.J., Kim, M.S., Choi, H.S. and Jung, S.J.: Protective immunity induced by ankyrin repeat-containing protein-based DNA vaccine against rock bream iridovirus (RBIV) in rock bream (*Oplegnathus fasciatus*). *Virus Research*, 198827, 2022.
- Kwon, M.G., Kim, J.W., Park, M., Hwang, J.Y., Choi, H.S., Kim, M.C., Park, D.W., Jung, J.M. and Park, C.I.: Microarray analysis of gene expression in peripheral blood leucocytes from rock bream (*Oplegnathus fasciatus*) after stimulation by LPS, ConA/PMA, and poly I:C. *Genes. Genomics*, 35: 343-353, 2013.
- Jung, M.H., Chico, V., Ciordia, S., Mena, M.C., Jung, S.J. and Ortega-Villaizan, M.D.M.: The Megalocytivirus RBIV induces apoptosis and MHC Class I presentation in rock bream (*Oplegnathus fasciatus*) red blood cells. *Frontiers in Immunology*, 10: 160, 2019.
- Kim, A., Yoon, D., Lim, Y., Roh, H.J., Kim, S., Park, C.I., Kim, H.S., Cha, H.J., Choi, Y.H. and Kim, D.H.: Co-expression network analysis of spleen transcriptome in rock bream (*Oplegnathus fasciatus*) naturally infected with rock bream iridovirus (RBIV). *Int J Mol Scien*, 21: 1707, 2020.
- Jung, M.H., Nikapitiya, C., Song, J.Y., Lee, J.H., Lee, J., Oh, M.J. and Jung, S.J.: Gene expression of pro- and anti-apoptotic proteins in rock bream (*Oplegnathus fasciatus*) infected with *Megalocytivirus* (family *Iridoviridae*). *Fish. Shellfish Immunol*, 37: 122-130, 2014.
- Nikapitiya, C., Jung, S.J., Jung, M.H., Song, J.Y., Lee, J., Lee, J.H. and Oh, M.J.: Identification and Molecular Characterization of Z/ZE Lineage MHC Class I Heavy Chain Homologue and β 2-microglobulin from Rock Bream *Oplegnathus fasciatus*. *Fish. Pathol*, 49: 93-112, 2014.
- Jung, M.H. and Jung, S.J.: Gene expression regulation of the TLR9 and MyD88-dependent pathway in rock bream against rock bream iridovirus (RBIV) infection. *Fish. Shellfish Immunol*, 70: 507-514, 2017b.
- Jung, M.H. and Jung, S.J.: CpG ODN 1668 induce innate and adaptive immune responses in rock bream (*Oplegnathus fasciatus*) against rock bream iridovi-

- rus (RBIV) infection. *Fish. Shellfish Immunol*, 69: 247-257, 2017c.
- Jung, M.H. and Jung, S.J.: Innate immune responses against rock bream iridovirus (RBIV) infection in rock bream (*Oplegnathus fasciatus*) following poly (I:C) administration. *Fish. Shellfish Immunol*, 71: 171-176, 2017cd.
- Do, J.W., Moon, C.H., Kim, H.J., Ko, M.S., Kim, S.B., Son, J.H., Kim, J.S., An, E.J., Kim, M.K., Lee, S.K., Han, S.K., Cha, S.J., Park, M.S., Park, M.A., Kim, Y.C., Kim, J.W. and Park, J.W.: Complete genomic DNA sequence of rock bream iridovirus. *Virology*, 325: 351-363, 2004.
- Caipang, C.M.A., Takano, T., Hirono, I. and Aoki, T.: Genetic vaccines protect red seabream, *Pagrus major*, upon challenge with red seabream iridovirus (RSIV). *Fish. Shellfish Immunol*, 21: 130-138, 2006.
- Fu, X., Li, N., Lin, Q., Guo, H., Zhang, D., Liu, L. and Wu, S.: Protective immunity against infectious spleen and kidney necrosis virus induced by immunization with DNA plasmid containing mcp gene in Chinese perch *Siniperca chuatsi*. *Fish. Shellfish Immunol*, 40: 259-266, 2014.
- Thanasaksiri, K., Hirono, I., and Kondo, H.: Temperature-dependent regulation of gene expression in poly (I:C)-treated Japanese flounder, *Paralichthys olivaceus*. *Fish. Shellfish Immunol*, 45: 835-840, 2015.
- Cho, H.K., Kim, J., Moon, J.Y., Nam, B.H., Kim, Y.O., Kim, W.J., Park, J.Y., An, C.M., Cheong, J. and Kong, H.J.: Microarray analysis of gene expression in olive flounder liver infected with viral haemorrhagic septicaemia virus (VHSV). *Fish. Shellfish Immunol*, 49: 66-78, 2016.
- Romero, A., Forn-Cuní, G., Moreira, R., Milan, M., Bargelloni, L., Figueras, A. and Novoa, B.: An immune-enriched oligo-microarray analysis of gene expression in Manila clam (*Venerupis philippinarum*) haemocytes after a *Perkinsus olseni* challenge. *Fish. Shellfish Immunol*, 43: 275-286, 2015.
- Lua, D.T., Yasuike, M., Hirono, I. and Aoki, T.: Transcription program of red sea bream iridovirus as revealed by DNA microarrays. *J. Virol.* 79: 15151-15164, 2005.
- Lua, D.T., Yasuike, M., Hirono, I., Kondo, H. and Aoki, T.: Transcriptional profile of red seabream iridovirus in a fish model as revealed by viral DNA microarrays, *Virus genes*. 35 (2007) 449-461.
- Teng, Y., Hou, Z., Gong, J., Liu, H., Xie, X., Zhang, L., Chen, X. and Qin, Q.W.: Whole-genome transcriptional profiles of a novel marine fish iridovirus, Singapore grouper iridovirus (SGIV) in virus-infected grouper spleen cell cultures and in orange-spotted grouper, *Epinephelus coioides*. *Virology*, 377: 39-48, 2008.
- Livak, K.J. and Schmittgen, T.D.: Analysis of relative gene expression data using real time quantitative PCR and the 2⁻(Delta Delta C(T)) Method. *Methods*, 25: 402-408, 2001.
- Bennett, V.: Ankyrins. Adaptors between diverse plasma membrane proteins and the cytoplasm. *J Biol Chem*. 267: 8703-8706, 1992.
- He, J.G., Deng, M., Weng, S.P., Li, Z., Zhou, S.Y., Long, Q.X. and Chan, S.M.: Complete genome analysis of the mandarin fish infectious spleen and kidney necrosis iridovirus. *Virology*, 291: 126-139, 2001.
- Herbert, M.H., Squire, C.J. and Mercer, A.A.: Poxviral ankyrin proteins. *Viruses*, 7: 709-738, 2015.
- Lu, Z., Li, Y., Zhang, Y., Kutish, G.F., Rock, D.L. and Van Etten, J.L.: Analysis of 45 kb of DNA located at the left end of the chlorella virus PBCV-1 genome. *Virology*, 206: 339-352, 1995.
- Raoult, D., Audic, S., Robert, C., Abergel, C., Renesto, P., Ogata, H. and Claverie, J. M.: The 1.2-megabase genome sequence of Mimivirus. *Science*. 306: 1344-1350, 2004.
- Bitra, K., Suderman, R.J. and Strand, M.R.: Polydnavirus Ank proteins bind NF-kappaB homodimers and inhibit processing of Relish. *PLoS Pathog*, 8: e1002722, 2012.
- Bin, L., Li, X., Feng, J., Richers, B. and Leung, D.Y.: Ankyrin Repeat Domain 22 Mediates Host Defense Against Viral Infection Through STING Signaling Pathway. *J Immunol*, 196: 201-204, 2016.
- Ink, B.S., Gilbert, C.S. and Evan, G.I.: Delay of vaccinia virus-induced apoptosis in nonpermissive Chinese hamster ovary cells by the cowpox virus CHOhr and adenovirus E1B 19K genes. *J Virol*, 69: 661-668, 1995.
- Revilla, Y., Callejo, M., Rodriguez, J.M., Culebras, E., Nogal, M.L., Salas, M. L. and Fresno, M.: Inhibition of nuclear factor kappaB activation by a virus-encoded Ikb-like protein. *J Biol Chem*, 273: 5405-5411, 1998.
- Cunningham, C., Davison, A.J., Dolan, A., Frame, M.C., McGeoch, D.J., Meredith, D.M. and Orr, A. C.: The UL13 virion protein of herpes simplex virus type 1 is phosphorylated by a novel virus-induced protein kinase. *J Gen Virol*, 73: 303-311, 1992.
- Overton, H.A., McMillan, D.J., Klavinskis, L.S., Hope, L., Ritchie, A.J. and Wong-Kai-In, P.: Herpes sim-

- plex virus type 1 gene UL13 encodes a phosphoprotein that is a component of the virion. *Virology*, 190: 184-192, 1992.
- Paterson, T. and Everett, R.D.: Mutational dissection of the HSV-1 immediate-early protein Vmw175 involved in transcriptional transactivation and repression. *Virology*, 166: 186-196, 1988.
- Mayer, U., Nischt, R., Pöschl, E., Mann, K., Fukuda, K., Gerl, M. and Timpl, R.: A single EGF-like motif of laminin is responsible for high affinity nidogen binding. *The EMBO Journal*, 12: 1879-1885, 1993.
- Takano, T., Matsuyama, T., Kawato, Y., Sakai, T., Kurita, J., Matsuura, Y. and Nakayasu, C.: Identification of the Epitope Recognized by the Anti-Red Sea Bream Iridovirus (RSIV) Monoclonal Antibody M10 Using a Phage Display RSIV Peptide Library. *Fish Pathol*, 54: 83-92, 2020.
- Xu, X., Weng, S., Lin, T., Tang, J., Huang, L., Wang, J. and He, J.: VP23R of infectious spleen and kidney necrosis virus mediates formation of virus-mock basement membrane to provide attaching sites for lymphatic endothelial cells. *J Virol*, 84: 11866-11875, 2010.
- Xu, X., Yan, M., Wang, R., Lin, T., Tang, J., Li, C. and He, J. G.: VP08R from infectious spleen and kidney necrosis virus is a novel component of the virus-mock basement membrane. *J Virol*, 88: 5491-5501, 2014.

Manuscript Received : Nov 09, 2022

Revised : Nov 28, 2022

Accepted : Dec 06, 2022